



저작자표시-비영리-변경금지 2.0 대한민국

이용자는 아래의 조건을 따르는 경우에 한하여 자유롭게

- 이 저작물을 복제, 배포, 전송, 전시, 공연 및 방송할 수 있습니다.

다음과 같은 조건을 따라야 합니다:



저작자표시. 귀하는 원저작자를 표시하여야 합니다.



비영리. 귀하는 이 저작물을 영리 목적으로 이용할 수 없습니다.



변경금지. 귀하는 이 저작물을 개작, 변형 또는 가공할 수 없습니다.

- 귀하는, 이 저작물의 재이용이나 배포의 경우, 이 저작물에 적용된 이용허락조건을 명확하게 나타내어야 합니다.
- 저작권자로부터 별도의 허가를 받으면 이러한 조건들은 적용되지 않습니다.

저작권법에 따른 이용자의 권리는 위의 내용에 의하여 영향을 받지 않습니다.

이것은 [이용허락규약\(Legal Code\)](#)을 이해하기 쉽게 요약한 것입니다.

[Disclaimer](#)

치의과학박사 학위논문

Angelica tenuissima Nakai: Promotion
of Osteo/Odontoblastic Differentiation
of Human Periodontal Ligament Stem
Cells and Antiviral Property
against Influenza Virus, *in vitro*

한고본: 사람치주인대 줄기세포의
조골세포/조상아세포 분화 촉진 효과
및 인플루엔자 바이러스에 대한
항바이러스 성질, 시험관 내 연구

2020년 8월

서울대학교 대학원

치의과학과 구강악안면외과학 전공

박 원 중

ABSTRACT

Angelica tenuissima Nakai: Promotion
of Osteo/Odontoblastic Differentiation of
Human Periodontal Ligament Stem Cells
and Antiviral Property
against Influenza Virus, *in vitro*

Won-Jong Park, D.D.S., M.S.D.

Program in Oral and Maxillofacial Surgery

Department of Dental Science

The Graduate School

Seoul National University

Directed by Prof. Pill-Hoon Choung, D.D.S., M.S.D., Ph.D.

Objectives

Angelica tenuissima Nakai (ATN) is a herbal medicine used in the treatment of toothache, headaches, and cold symptoms. Published research to date has not systematically explored the therapeutic effects of ATN. The purpose of this study is to investigate the effects of ATN on alleviating toothache and cold symptoms.

Methods

Effects of ATN on the proliferation and differentiation of hPDLSCs were evaluated using MTT assay, Alizarin red S staining, real-time PCR and western blotting. The roles of ATN during dentin-like structure formation was investigated using hPDLSCs mixed with treated dentin matrix either with or without ATN. An animal study was, additionally, performed with subcutaneous cell suspension and scaffold transplantation into immunocompromised mice.

For determining the antiviral property of ATN against influenza virus (H1N1, H3N2), time of addition assay, microscopic examination, influenza virus-ATN binding assay and real-time PCR were performed.

Results

Angelica tenuissima Nakai promoted osteo/odontoblastic differentiation of hPDLSCs, accelerated mineral nodule formation *in vitro* and displayed no toxicity at higher concentrations. The mRNA expression levels of ALP, COL1, OPN, DMP1, DSPP in hPDLSCs, and the

protein levels of OCN, DSPP, DMP1, Runx2 were significantly increased with ATN treatment. Osterix (OSX) gene overexpressed-HEK 293 cells, treated with ATN (100 µg/ml), showed an increase in BSP promoter activity. No apparent osteogenesis was observed in both control and experimental groups *in vivo*.

Antiviral properties of ATN were observed against the H1N1 and H3N2 viruses. Microscopy also confirmed an increased survival rate of the host cells. The addition of ATN before virus adsorption showed similar results with whole period treatment. The pre-treated group and co-treated group showed a lower level of viral RNA (M1 protein).

Conclusion

The results of this study suggest that ATN promotes osteo/odontoblastic differentiation of hPDLSCs and has an antiviral property against influenza virus. These therapeutic properties of ATN can serve as the theoretical basis for further research on the applicability of ATN in periodontal tissue regeneration and antiviral agent development.

Keywords: *Angelica tenuissima* Nakai, human periodontal ligament stem cells, osteoblastic/odontoblastic differentiation, antiviral, influenza virus

Student Number:2011-31174

CONTENTS

ABSTRACT	j
CONTENTS	iv
LIST OF FIGURES	v
I. INTRODUCTION	1
II. MATERIALS AND METHODS	4
III. RESULTS	15
IV. DISCUSSION	34
V. CONCLUSIONS	39
VI. REFERENCES	40
VII. ABSTRACT IN KOREAN	48

LIST OF FIGURES

Figure 1. Characterization and multi-lineage differentiation of human periodontal ligament stem cells(hPDLSCs).....	16
Figure 2. ATN does not affect on the proliferation/migration of hPDLSCs.....	18
Figure 3. ATN increases mineralized nodule formation of hPDLSCs..	20
Figure 4. ATN enhances the <i>in vitro</i> expression of osteo/odontoblastic differentiation markers in hPDLSCs.....	22
Figure 5. ATN enhances the <i>in vitro</i> expression of osteo/odontoblastic differentiation markers in hPDLSCs	23
Figure 6. ATN showed no significant effects on osteo/odontoblastic differentiation of hPDLSCs <i>in vivo</i>	25
Figure 7. Cytotoxicity of ATN in MDCK cells	27
Figure 8. ATN has antiviral property against influenza viruses of subtypes H1N1 and H3N2.....	29

Figure 9. ATN increases the survival rate of cells infected with influenza (H1N1, H3N2) viruses.....	30
Figure 10. ATN exhibits antiviral activity at an early stage in a time-of-addition assay.....	32
Figure 11. ATN inhibits viral RNA synthesis at an early stage of infection.....	33

I. INTRODUCTION

Angelica tenuissima Nakai (ATN), belonging to the *Umbelliferae* family, is a traditional medicine used to treat headaches, toothache, and cold symptoms in the East Asian countries (1, 2). Hepatoprotective and antioxidative activities of ATN are well-studied (3, 4), and its anti-inflammatory role as a cyclooxygenase-2 inhibitor has also been reported (2). The anti-inflammatory properties of ATN are due to its components that include ferulic acid and various essential oil compounds, such as limonene, 3-butyldenephthalide, γ -terpinene, ligustilide, senkyunolide, and neocnidilide (5–7). Ferulic acid has been shown to neutralize lipopolysaccharide-induced inflammatory response (8). Ligustilide prevents osteoarthritis by suppressing NF- κ B activation through the PI3K/AKT pathway (9).

A common cause of toothache is pulp tissue inflammation associated with periodontal diseases. Dental caries leads to dental pulp inflammation, also known as acute pulpitis, and induces a severe pulp pain (10). Damaged teeth restore function and appearance relatively well after endodontic and restorative treatment. Periodontitis is one of the most common chronic inflammatory diseases which results in the destruction of periodontal tissues (11). Treatment of periodontitis involves not only preventing infection but also regenerating damaged periodontal tissue, including the alveolar bone, the cementum, and the periodontal ligament. Routine treatments for periodontal disease include basic treatment, guided tissue regeneration (GTR), and guided bone regeneration (GBR) (12). The outcomes of these methods are limited and are often associated with poor clinical predictability. From this point of view, stem cell

therapy has been studied and has shown improved clinical outcomes (13, 14). Human periodontal ligament stem cells (hPDLSCs) represent one of the most reliable sources of mesenchymal stem cells (MSCs) that have the potential to differentiate into bone, periodontal ligament (PDL), and cementum-forming lineages (15). These cells display self-renewal and multipotential abilities that are useful in periodontal tissue treatment therapies and regenerative medicine applications (13, 16, 17).

The destruction of periodontal tissue in periodontitis is due to inflammatory reactions caused by bacterial infections. Thus, anti-inflammatory property of ATN can play an important role in the treatment of periodontitis. It has been shown that the anti-inflammatory effect of ATN is based on cyclooxygenase-2 suppression (2). However, no studies have focused on the effect of ATN on the regeneration of periodontal tissues.

Influenza viruses have segmented negative-sense RNA genome which encode virus proteins. hemagglutinin (HA) and neuraminidase (NA) are the best-characterized viral proteins that categorize influenza A virus into different strains (18). Influenza A viruses have been evolving and circulating among their animal and human hosts ever since the pandemic influenza outbreak in 1918 that caused substantial mortality and morbidity.

At present, vaccines and antiviral drugs are used for the prevention and treatment of influenza (19, 20). Currently, the application of two types of antiviral agents known as M2 channel inhibitors and neuraminidase inhibitors, are available for the treatment of influenza (21). However, use of these drugs is limited by the emergence of drug-resistant viruses (22, 23). Many studies have

focused on developing naturally-derived anti-influenza agents and traditional herbal medicines (24). Although ATN has been used to alleviate flu-like symptoms, no specific mechanism against the virus has been identified.

This study investigates the effect of ATN on periodontal tissue regeneration and examines the antiviral scope of ATN in the treatment of influenza virus infection, with the aim to understand the usability of ATN for the management of periodontal disease and influenza infection.

II. MATERIAL AND METHODS

1. Preparation of *Angelica tenuissima* Nakai extract

ATN was purchased from Kwang Myung Dang (Ulsan, Korea) and its authenticity was verified at the Department of Herbology, College of Korean Medicine, Wonkwang University. Extraction was performed using the following method. After adding 1000 mL distilled water to 75 g of ATN, the mixture underwent decoction for 2 h at 100°C, followed by enrichment and freeze-drying process to obtain the ATN extract. The yield of the dried extract was 13.7 g

2. Preparation of hPDLSCs

hPDLSCs were isolated from human third molar. Experiments were conducted using teeth obtained from healthy young male over the age of 20. The protocol was approved by the Institutional Review Board of the Wonkwang University Dental Hospital, Iksan, South Korea (IRB No. WKDIRB-201708-02). hPDLSCs were isolated from the root surface using a scalpel. The separated tissues were digested in the alpha-modification of Eagle's medium (α -MEM; Gibco BRL, Grand Island, NY) containing 4 mg/mL dispase (Boehringer, Mannheim, Germany) and 3 mg/mL collagenase type I (Worthington Biochem, Freehold, NJ) for 1 h at 37°C. Single-cell suspensions were obtained by passing the mixture through a strainer pore size of 70 μ m strainer (Falcon BD Labware, Franklin Lakes, NJ). The cells were cultured in 100 mm dish with α -MEM containing 10 % fetal bovine serum

(Gibco BRL), 100 μ M L-ascorbic acid 2-phosphate (Sigma-Aldrich, St. Louis, MO), 2 mM L-glutamine (Gibco BRL), 100 U/ml penicillin, and 100 μ g/ml streptomycin (Biofluids, Rockville, MD) at 37°C in 5% CO₂. The third or forth passage of cells was used for the experiment.

3. Flow cytometric analysis

The immunophenotype of hPDLSCs was characterized by flow cytometry. The expression of mesenchymal stem cell-associated surface markers at passage 3 was analyzed. Cells in their third passage (1.0×10^6 cells) were suspended in phosphate-buffered saline (PBS) containing 2 % fetal bovine serum (Gibco BRL) for 30 min for blocking. Cells were then incubated with antibodies specific to CD34, CD13, CD90, or CD146 at 4°C for 2 h. All antibodies were purchased from BD Biosciences (San Jose, CA). Flow cytometry was carried out using the FACS Calibur flow cytometer (Becton Dickinson Immunocytometry Systems, San Jose, CA). The percentage of CD13⁺, CD90⁺, CD146⁺ and CD34⁻ cells was measured.

4. Osteogenic, chondrogenic and adipogenic differentiation

To evaluate osteogenic, chondrogenic, and adipogenic differentiation, cells were cultured in StemPro Osteogenesis, StemPro Chondrogenesis, and StemPro Adipogenesis differentiation medium (Gibco BRL), respectively, with the appropriate supplements. At week 3, the cells were washed with PBS and fixed in 3.7 % paraformaldehyde for 10 min. The cells were stained with 2 %

Alizarin red S stain (Sigma-Aldrich), 1 % Alcian Blue (Sigma-Aldrich), and 0.3 % Oil Red O dye (Sigma-Aldrich) to detect osteogenic, chondrogenic, and adipogenic differentiation. Cells were visualized under a light microscope.

5. Cell proliferation/cytotoxicity and migration assay

Cytotoxicity of ATN was evaluated using the 3-(4,5-dimethylthiazol-2-yl)-2,5-diphenyltetrazolium bromide (MTT) assay. hPDLSCs cells were cultured for 24 and 72 h in a 96-well plate containing various concentrations of ATN. After adding 20 μ L of MTT (5 mg/mL) solution into a 96-well plate, cells were incubated for 1h. The supernatant was removed, and isopropanol (100 μ L) was added. The solubilized MTT crystals were quantitatively analyzed by measuring the absorbance at 490 nm using SpectraMax 190 (Molecular Devices, San Jose, CA).

To observe the effects of ATN on cell motility and hPDLSC migration, wound healing assays were performed on hPDLSC monolayers. Cells were allowed to grow to 90 % confluence in 6-well plate. Cell monolayers were wounded with a plastic tip (1 mm). Cell debris was removed by washing twice with PBS and then incubated either with ATN (100 μ g/ml) or without ATN. Cell migration into the wound surface was examined under microscopy at 0, 12, 18, and 24 h.

6. Alizarin red S staining

Cells were cultured in 24-well plates in α -MEM containing 10 % FBS at an initial density of 4×10^4 cells/well until reaching 50–60 % confluence. For mineralization, the hPDLSCs were cultured in osteogenic differentiation medium with 50 μ g/ml ascorbic acid, 10 mM β -glycerophosphate, and 100 nM dexamethasone (Sigma–Aldrich) for 2 weeks. At week 2 the accumulation of mineral nodules was detected by staining with 2 % Alizarin red S (Sigma Aldrich) at pH 4.2. For measuring calcium content, the cells were destained by adding 3 ml of 10 mM sodium phosphate in 10 % acetylpyrimidium (pH 7.0) solution to each stained well, followed by a 15-min incubation at room temperature. The destained samples were transferred to a 96-well plate and their absorbances were measured at 562 nm.

7. Western blot analysis

hPDLSCs (1.0×10^6 cells/dish) were cultured in osteogenic differentiation media with ATN (100 μ g/ml) or without ATN. for 2 weeks. Cell lysate protein concentrations were determined using the DC Protein Assay Kit (Bio–Rad Laboratories, Hercules, CA). Equal amounts of protein (30 μ g/lane) were resolved by SDS–PAGE and transferred to a polyvinylidene difluoride membrane (GE Healthcare, Buckinghamshire, UK). Primary antibodies against runt–related transcription factor 2 (Runx2), α -tubulin (Cell Signaling Technology, Danvers, MA), bone sialoprotein (BSP), osteopontin (OPN), osteocalcin

(OCN), dentin sialophosphoprotein (DSPP), and dentin matrixprotein 1 (DMP1) (Santa Cruz Biotechnology, Santa Cruz, CA) were used. Blots were developed using horseradish peroxidase-conjugated secondary antibodies (Cell Signaling Technology) and visualized using an enhanced chemiluminescence kit (GE Healthcare).

8. RNA preparation and real-time PCR analysis

To evaluate gene expression levels in ATN-induced differentiated hPDLSCs, 1.0×10^6 cells were seeded in a 60-mm culture dish and cultured for 2 weeks under osteogenic differentiation induction conditions. Total RNA was prepared using an RNeasy Mini Kit (Qiagen, Valencia, CA). Oligo (dT) primers and reverse transcriptase (Takara, Nojihigashi, Japan) were used to synthesize the cDNA. Real-time PCR was performed using the SYBR Premix Ex Taq kit (Takara) on a StepOne™ Real-Time PCR System (Molecular Devices). Samples were incubated at 95°C for 30 s followed by 40 cycles at 95°C for 5 s and 60°C for 30 s. The expression level of GAPDH (glyceraldehyde-3-phosphate dehydrogenase) was used as an internal control to normalize mRNA expression. The ΔC_t was determined by subtracting the C_t value of GAPDH from that of the target. The relative expression levels of each gene were calculated using the $2^{-\Delta\Delta C_t}$ method. The specific primer sets used for this analysis are listed in Table 1.

9. Luciferase reporter assays

A luciferase reporter plasmid containing the promoter for the bone sialoprotein(BSP-Luc), a pCMV- β -gal plasmid, and a combination of OSX expression plasmids were transfected into HEK 293 cells. Transfected cells were treated with ATN (100 μ g/ml) or without ATN for 24 h and then lysed for the assessment of luciferase activity using Luciferase Reporter Assay Kit (Promega, Madison, WI). The transfection efficiency was normalized using β -galactosidase.

10. Evaluation of ATN effect on hPDLSCs *in vivo*

To study the effects of ATN on dentin-like structure formation *in vivo*, hPDLSCs (1.0×10^7 cells) were mixed with treated dentin matrix (TDM), either with ATN (100 μ g/ml) or without ATN. The human TDM, used as an inductive scaffold, was fabricated according to a previously reported protocol (25). The suspended cells were then transplanted subcutaneously into immunocompromised mice (n=6) (BALB/c-nu). For histological analysis, samples were obtained 8 weeks after transplantation and fixed in 3.7% paraformaldehyde solution made from 95% paraformaldehyde powder (Sigma-Aldrich) diluted in PBS for 48 h at 4°C, followed by their decalcification using 12 % EDTA (pH 7.4) at 4°C. The decalcified samples were embedded in paraffin and cut serially. Semi-serial 5- μ m sections were prepared for hematoxylin and eosin (H&E) staining. Stained sections were examined under a light microscope.

11. Propagation of Influenza virus in Madin - Darby canine kidney (MDCK) cell line

Influenza A/H1N1/2009/CA was provided by the Korea Centers for Disease Control and Prevention. Influenza A/H3N2 isolated from humans in 2014 was donated by the Korean National Research Resource Center (Seoul, Korea) (registration number: KBPV-VR-85). Madin - Darby canine kidney (MDCK) cells were grown in Dulbecco's modified Eagle's medium (DMEM) (Gibco BRL) supplemented with 2 mM of L-glutamine, 0.1 mM non-essential amino acid mixture, 100 U/ml penicillin, 100 µg/ml streptomycin (Biofluids) and 10% FBS (Gibco BRL). All cells were cultured as monolayers and incubated at 37°C in 5% CO₂.

12. Hemagglutination assay

Influenza viruses of the H1N1 and H3N2 subtypes, cultured in MDCK cells, were used to check the effectiveness of ATN. To compare the titer of Influenza virus, a Hemagglutination assay was used. A round-bottomed 96-well dish was prepared as follows: in the first column of the plate, 50 µl of virus sample was added; wells in the subsequent columns were filled with 2-fold serially diluted samples. After adding serial dilutions of the virus samples, 50 µl of 0.5 % chicken red blood cells were added to each well and mixed gently. The plate was incubated for 30 min at room temperature. Following

the incubation period, the assay was analyzed to distinguish between agglutinated and non-agglutinated wells.

13. Determination of Influenza a Virus TCID₅₀

The influenza virus was 10-fold diluted and added to a 96-well plate, which contained 2×10^4 MDCK cells/well. Infected cells were incubated at 37 °C for 72 h. The endpoint was determined when the CPE appeared. The titer was calculated using the Reed - Muench method.

14. Influenza virus - ATN binding assay

The attachment between virus and ATN and was evaluated using a binding assay. Influenza virus H1N1 or H3N2 (MOI = 0.5) was pre-incubated with ATN (0.8 to 100 µg/mL) at 4 °C for 1 h. The titer of ATN-treated virus was determined using a hemagglutination assay.

15. Time-of-addition assay

MDCK cells in 6-well plates were infected with influenza virus H1N1 (MOI = 0.5) between - 1 and 0 h for 1 h. The cells were then treated with ATN (100 µg/mL) at five different intervals: -3 to -1 h (pretreatment), -3 to 9 h (whole period treatment), 0 to 9 h, 3 to 9 h, and 6 to 9 h post-infection (pi). The supernatants were harvested at 9 h pi. the Viral titer was determined using a TCID₅₀ assay protocol.

16. Microscopic examination of virus infected cells

MDCK cells in 24-well plates were pretreated with various concentrations of ATN (50 - 800 µg/ml) for 2 h and then infected with influenza virus H1N1, H3N2 (MOI=0.5). Microscopic examination was performed at 24 h pi using a light microscope with 4X objective lens.

17. Evaluation of *In vitro* cytotoxicity of ATN

The cytotoxicity of ATN against MDCK cells was determined via MTT assay, which was performed for 48 h with various concentrations of ATN. The 50% cytotoxic concentration (CC₅₀) values were calculated using Prism 5.03 software (Graphpad Software, San Diego, CA).

18. Viral RNA isolation and real-time PCR

MDCK cells were infected with influenza virus H1N1, H3N2 (MOI=0.1) for 1 h, and treated with ATN (1 mg/ul) at the indicated period. Cells were harvested at 9 h pi. Real-time PCR was carried out same as described in the previous method. The primer sequences for M1 were 5' -GAC CAA TCC TGT CAC CTC-3' (forward) and 5' -GAT CTC CGT TCC CAT TAA GAG-3' (reverse). The GAPDH primers were 5' -AAG AAG GTG GTG AAG CAG GC-3' (forward) and 5' -TCC ACC ACC CTG TTG CTG TA-3' (reverse).

19. Statistical analysis

Statistical analysis was performed using Prism 5.03 software (Graphpad Software). One-way ANOVA with Tukey's post-hoc test was used. P values < 0.05 were considered statistically significant.

Table 1. Primer sequences for reverse transcription-polymerase chain reaction

Gene	GenBank No.	Sequences
ALP	NM007431	5'-CCAACCTCTTTTGTGCCAGAGA -3' 5'-GGCTACATTGGTGTTGAGCTTTT -3'
COL1	NM007742	5'-GCTCCTCTTAGGGGCCACT -3' 5'-CCACGTCTCACCATTGGGG -3'
OPN	J04765	5'-TGAAACGAGTCAGCTGGATG-3' 5'-TGAAATTCATGGCTGTGGAA -3''
DSPP	NM_014208	5'-GTGAGGACAAGGACGAATCTGA-3' 5'-CACTACTGTCACTGCTGTCACT-3'
DMP1	U89012	5'-ACAGGCAAATGAAGACCC-3' 5'-TTCCTGGCTTGTATGG-3'
GAPDH	NM_002046	5'-ACCACAGTCCATGCCATCA-3' 5'-TCCACCACCCTGTTGCTGT-3'

Abbreviations: ALP, alkaline phosphatase; Coll, type 1 collagen; OPN, osteopontin; DSPP, dentin sialophosphoprotein; DMP1, dentin matrix protein 1

III. RESULTS

1. Characterization and multi-lineage differentiation of hPDLSCs

To characterize the cultured hPDLSCs, the multi-lineage differentiation capacity of hPDLSCs was investigated *in vitro* with osteogenic, chondrogenic, and adipogenic medium. After 3 weeks of osteogenic, chondrogenic and adipogenic induction, hPDLSCs formed Alizarin red S-positive mineral deposits, Alcian Blue-positive nodules and Oil Red O-positive lipid droplets throughout the adherent layers (Fig. 1A). Flow cytometric analysis was performed using mesenchymal stem cell marker including CD13, CD90, and CD146. Flow cytometric analysis showed that 97.79% of hPDLSCs expressed CD13, 99.55% expressed CD90, 90.85% expressed CD146, and 0.18% expressed CD34 (Fig. 1B). The percentage of positive cells was determined by the relative intensity of antibody-binding cells. Putative positive markers of MSCs include CD13, CD90, and CD146 (26, 27), whereas CD34 is an MSC-negative marker that marks primitive hematopoietic progenitors and endothelial cells (28).

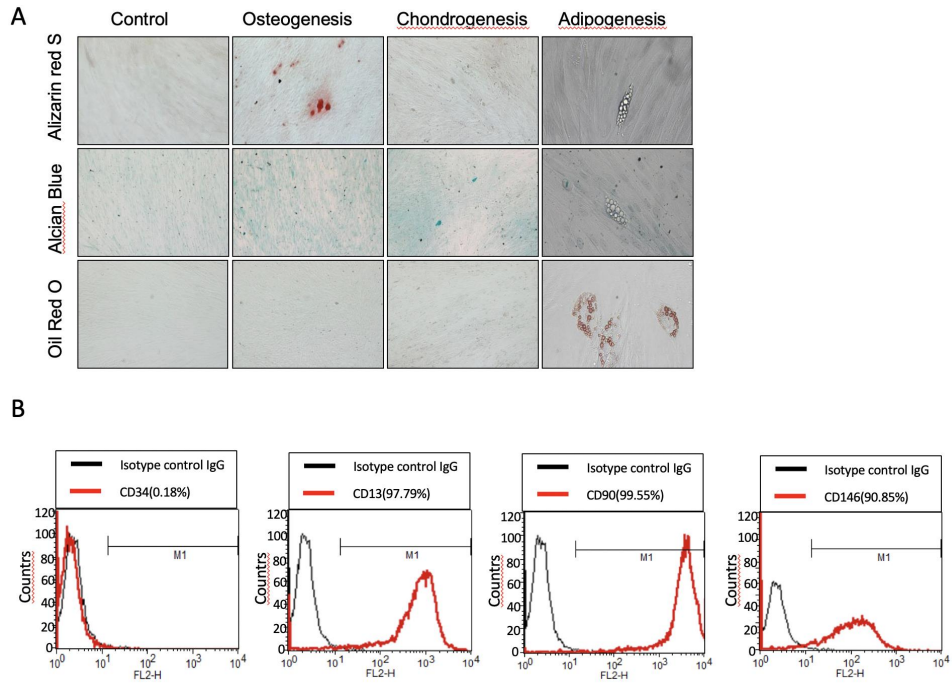


Figure 1. Characterization and multi-lineage differentiation of hPDLSCs.

(A) To investigate the multi-lineage differentiation potential of hPDLSCs, the cells were *in vitro* cultured in osteogenic, chondrogenic, and adipogenic differentiation media for 3 weeks. Alizarin red S staining, Alcian Blue staining and Oil red O staining respectively showed the progress of each group differentiation. (B) Flow cytometric analysis of hPDLSCs using mesenchymal stem cell markers, including CD13, CD34, CD90, and CD146. To analyze the populations of CD13⁺, CD90⁺, CD146⁺ and CD34⁻ cells was measured, the percentages of cells to the right of the M1 gate were measured (n=3).

2. ATN does not affect the proliferation/migration of hPDLSCs

To examine the effects of ATN on *in vitro* cell proliferation, hPDLSCs were treated with the indicated concentrations of ATN. After 24 and 72 h of culture, MTT cytotoxicity test was conducted. ATN displayed no toxicity at higher concentrations (Fig. 2B). To investigate whether ATN affects the migration of hPDLSCs, confluent monolayers were subjected to a wound-healing assay. Cells were cultured with or without ATN for 0, 12, 18, or 24 h, and the migration distances of the cells were measured. After 24 h, the ATN-treated cells showed no differences from the control group (Fig. 2A).

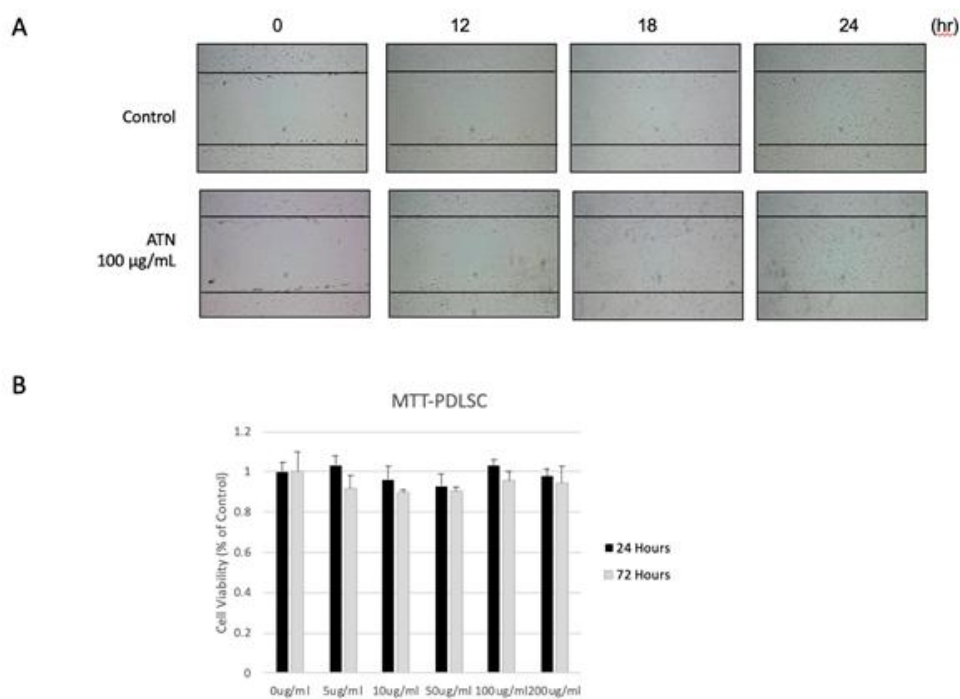


Figure 2. ATN does not affect the proliferation/migration of hPDLSCs.

(A) Wound - healing assays showed cellular migration of hPDLSCs. Confluent monolayers were wounded by scratching and then cultured in the absence or presence of ATN (100 $\mu\text{g/ml}$) for 0, 12, 18, and 24 h. (B) To determine the *in vitro* cytotoxicity of ATN, hPDLSCs were incubated with 0, 5, 10, 50, 100, and 200 $\mu\text{g/ml}$ of ATN for 24, 72 h.

3. ATN increases mineralized nodule formation of hPDLSCs

Human periodontal ligament mesenchymal stem cells (hPDLSCs) were cultured in osteogenic differentiation medium, with/without 25, 50, or 100 µg/ml of ATN. Treatment of hPDLSCs with 100 µg/ml ATN resulted in increased mineral nodules compared with the other treatments. The highest calcium contents were also observed in the 100 µg/ml ATN-treated group after the destaining of Alizarin red S (Fig. 3).

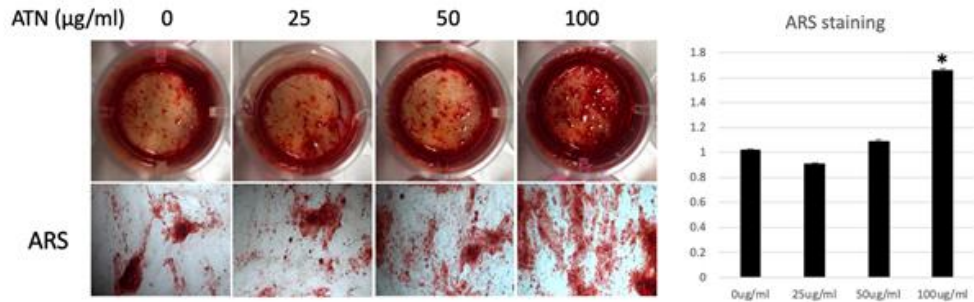


Figure 3. ATN increases mineralized nodule formation of hPDLSCs. Human periodontal ligament mesenchymal stem cells (hPDLSCs) were cultured for 14 days in osteogenic differentiation medium in the absence or presence of ATN (100 µg/ml). The effect of ATN on mineral nodule formation of hPDLSCs was determined by alizarin red S staining. The results of the destaining procedure showed higher calcium contents in the ATN-treated (100 µg/ml) group. *: $p < 0.05$ compared to the 0 µg/ml group (n=3).

4. ATN enhances the *in vitro* expression of osteo/odontoblastic differentiation markers in hPDLSCs

To investigate whether ATN induces osteo/odontoblastic differentiation of hPDLSCs, the expression levels of related genes were examined with real-time PCR. There was a significant increase in the mRNA expression levels of osteoblast- and odontoblast-associated markers, including ALP, COL1, OPN, DMP1, and DSPP when hPDLSCs were treated with ATN for 2 weeks (Fig. 4). In western blotting, ATN treated cells significantly increased the expression of OCN, DSPP, DMP1, and Runx2, and slightly increased the expression of BSP compared with the control group (Fig. 5A, B). BSP promoter activity showed an increased tendency for over-expression of OSX gene in HEK 293 cells treated with ATN (100 µg/ml) as compared with the control group (Fig. 5C). These results suggest that ATN promotes osteo/odontoblastic differentiation of hPDLSCs.

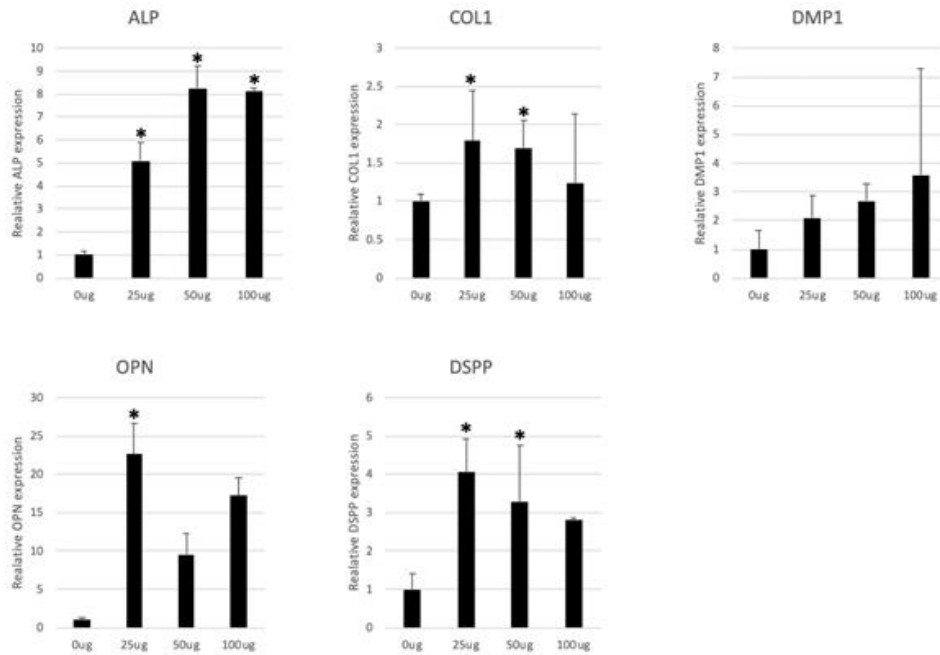


Figure 4. ATN enhances the *in vitro* expression of osteo/odontoblastic differentiation markers in hPDLSCs.

To investigate the effects of ATN on the differentiation of hPDLSCs, osteoblast- and odontoblast-associated genes were analyzed using real-time PCR. *: $p < 0.05$ compared to the 0 µg/ml group (n=3).

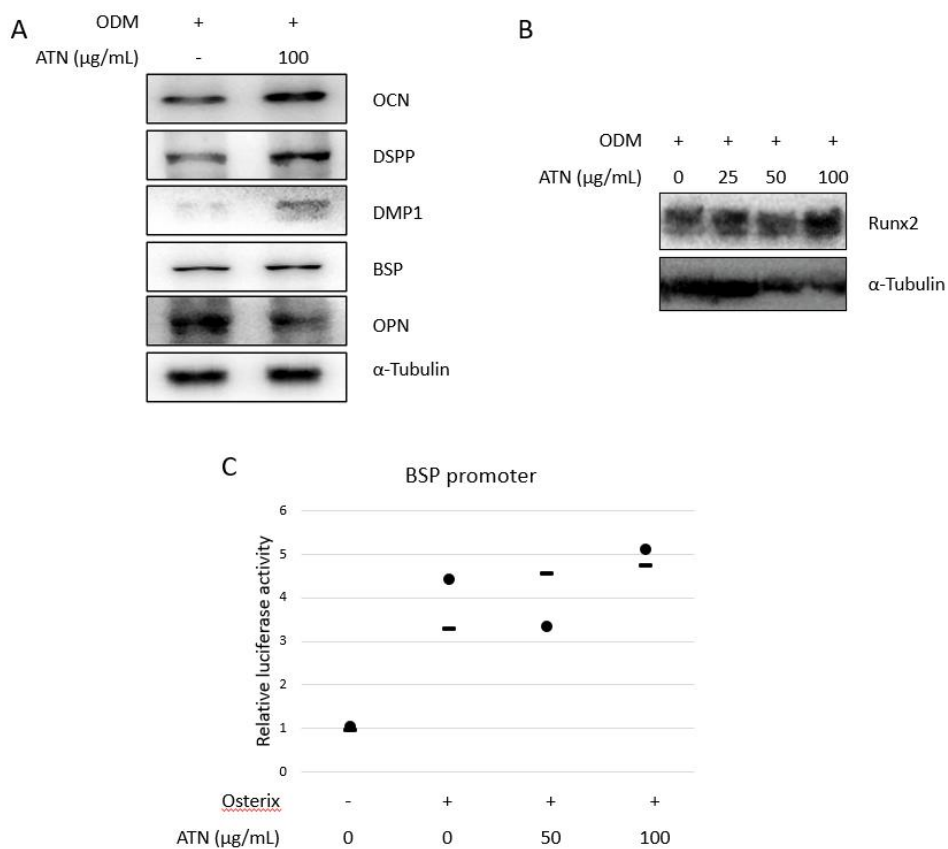


Figure 5. ATN enhances the *in vitro* expression of osteo/odontoblastic differentiation markers in hPDLSCs.

To investigate the effects of ATN on the differentiation of hPDLSCs, osteoblast- and odontoblast-associated genes were analyzed using western blot analysis (A, B). The BSP promoter assay was performed in OSX gene over-expressed HEK 293 cells with or without ATN (C).

5. ATN showed no significant effects on osteo/odontoblastic differentiation of hPDLSCs *in vivo*

To inspect the effects of osteo/odontoblastic differentiation and mineralized tissue formation *in vivo*, a transplantation model with treated dentin matrix (TDM) was used. After 8 weeks of transplantation, the transplanted mice were sacrificed. The ATN-treated samples showed no mineralization area and there were no significant differences from the control group. Multinucleated cells were observed around the TDM tissue, and absorption of some dentin matrix was also suspected in the ATN-treated samples (Fig. 6).

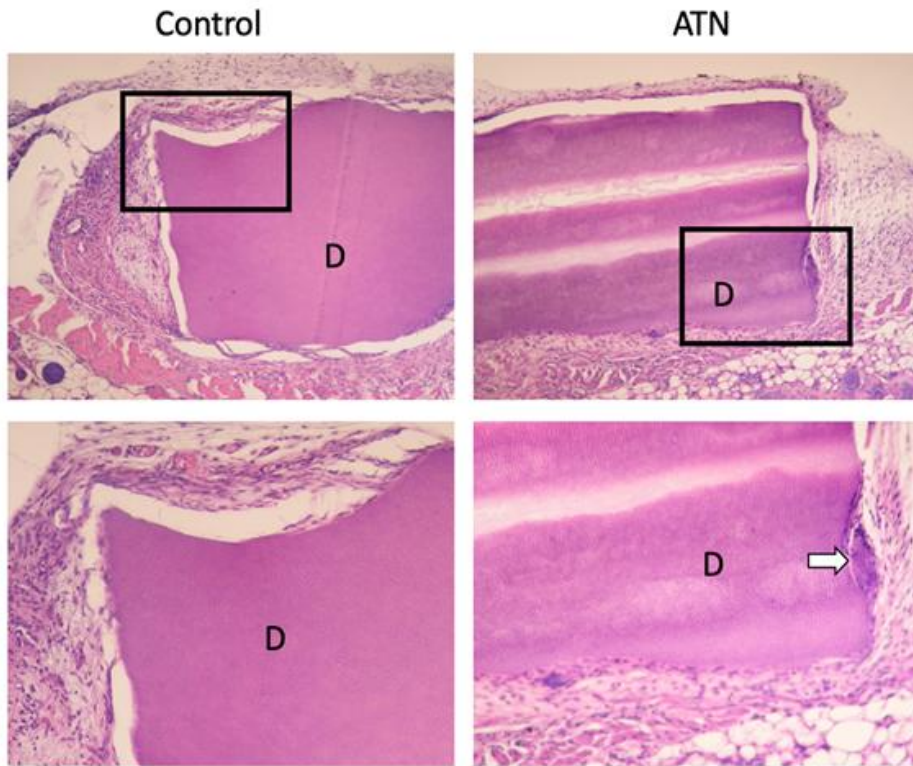


Figure 6. ATN showed no significant effects on osteo/odontoblastic differentiation of hPDLSCs *in vivo*.

H&E staining of treated dentin matrix (D) and transplanted tissue showed no significant differences between ATN-treated group and control group. Multinucleated cells were observed around the implanted tissue and absorption of some dentin was also suspected (white arrow).

6. Cytotoxicity of ATN in MDCK cells

MDCK cells were incubated in the presence of four fold ATN serial dilutions for 48 h. The viability of cells was then estimated using the MTT assay. As shown in Fig. 7, the CC₅₀ value was 4280 µg/ml.

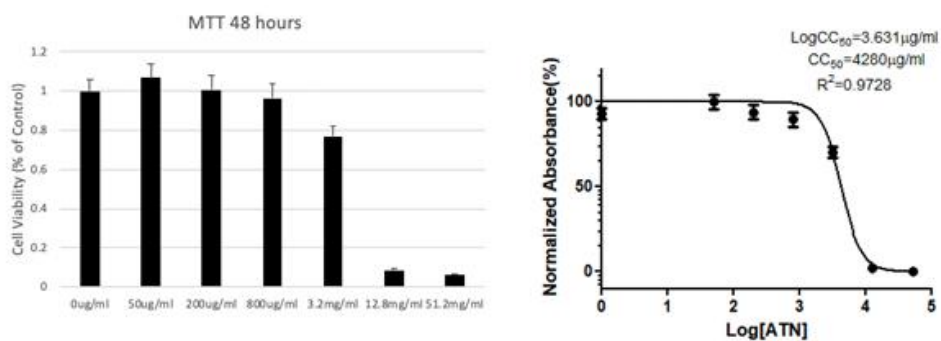


Figure 7. Cytotoxicity of ATN in MDCK cells.

MDCK cells were treated with serially diluted ATN (at concentrations as shown in the figure) and incubated for 48 h. The cell viability was determined using the MTT assay.

7. ATN has antiviral property against influenza viruses of subtypes H1N1 and H3N2

In this study, three ways to check the anti-influenza property of ATN were used. The first was to pretreat the MDCK cells with ATN for an hour and washing it off with PBS and then incubating the MDCK cells with virus. The second was to mix ATN and viruses and then incubated the mixture with MDCK cells. Third, after 1 h of infection, the supernatants were washed with PBS and treated with ATN. The concentration of the ATN was 50, 100, and 200 µg/ml and MOI was 0.1. All supernatants were collected at 24 h pi (post-infection) and the viral titer was determined using a hemagglutination assay. In the second and third methods, there were no differences from the control group, but in the first method, ATN showed antiviral properties. An inhibition of the virulence of the viruses was observed at ATN concentrations of 100 µg/ml and 200 µg/ml for H1N1, and 100 µg/ml for H2N2 (Fig. 8A). Microscopy also confirmed that more host cells survived when the MDCK cells was treated with ATN (100, 800 µg/ml) (Fig. 9).

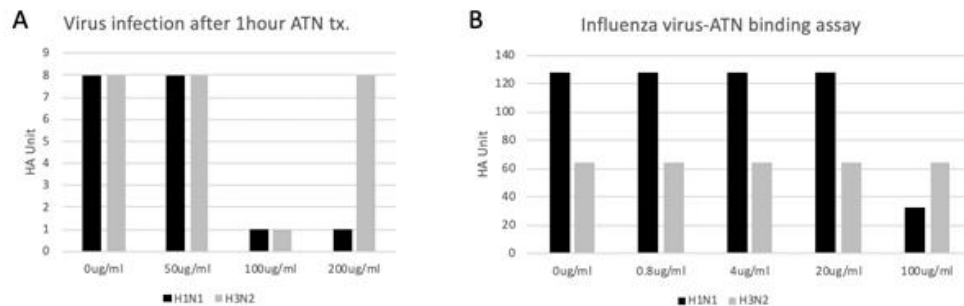


Figure 8. ATN has antiviral property against influenza viruses of subtypes H1N1 and H3N2.

(A) ATN showed inhibitory properties at concentrations of 100 and 200 $\mu\text{g/ml}$ for the H1N1 virus and at concentrations of 100 $\mu\text{g/ml}$ for the H3N2 virus. (B) Influenza virus-ATN binding assay shows that H1N1 is directly bound with ATN.

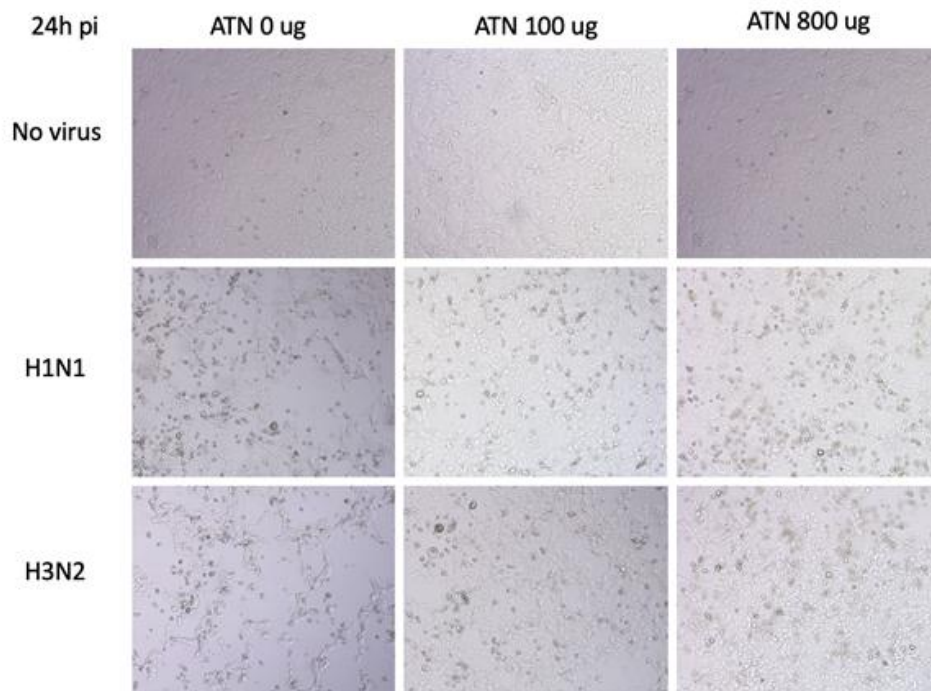


Figure 9. ATN increases the survival rate of cells infected with influenza (H1N1, H3N2) viruses.

MDCK cells infected with influenza viruses (MOI 0.5) were treated with ATN (100, 800 $\mu\text{g}/\text{ml}$). More cells survived when the virus was treated with ATN. Microscopic examination was done at 24 h pi using a microscope with 4X objective lens.

8. ATN exhibits antiviral activity at an early stage of infection

To explore the antiviral mechanism of ATN, a time-of-addition assay was performed. H1N1 was used to infect MDCK cells at MOI of 0.5. ATN was treated at six intervals (Fig. 10A). The results showed that the addition of ATN before virus adsorption (-3 to -1) showed similar results with whole period treatment (-3 to 9). In the results of the Influenza virus-ATN binding assay (Fig. 8B), HA unit of H1N1 was reduced at 100 µg/ml concentration, indicating the possibility that the ATN bound with the hemagglutinin (HA) of the H1N1 directly.

The effect of ATN in early stage was confirmed through the amount of intracellular viral RNA (M1 protein). The pre-treated group (-3 to -1) and co-treated group (-1 to 0) showed a lower level of viral RNA than the control group (Fig. 11B).

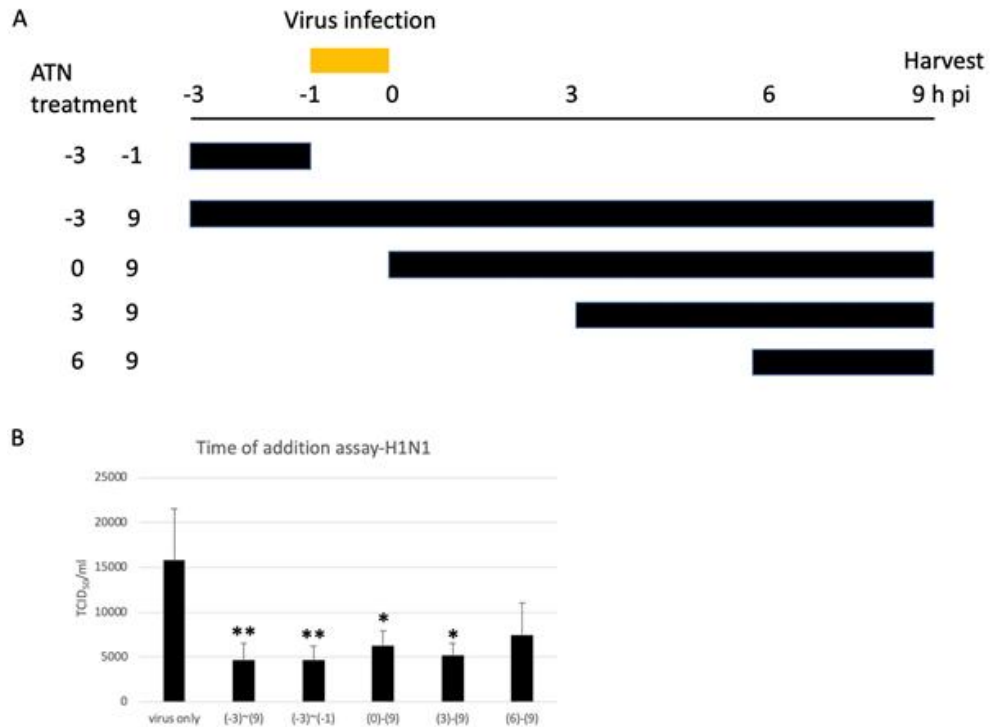


Figure 10. ATN exhibits antiviral activity at an early stage in a time-of-addition assay.

(A) Schematic diagram of ATN treatment. MDCK cells were infected with H1N1 (MOI = 0.5) at -1 to 0 h. ATN (100 μ g/ml) was incubated with the MDCK cells for the durations indicated. All supernatants were collected at 9 h pi to determine the titers using TCID₅₀. (B) The results show that ATN has an antiviral property. *: $p < 0.05$ compared to the virus only group (n=3); **: $p < 0.01$ compared to the virus only group (n=3).

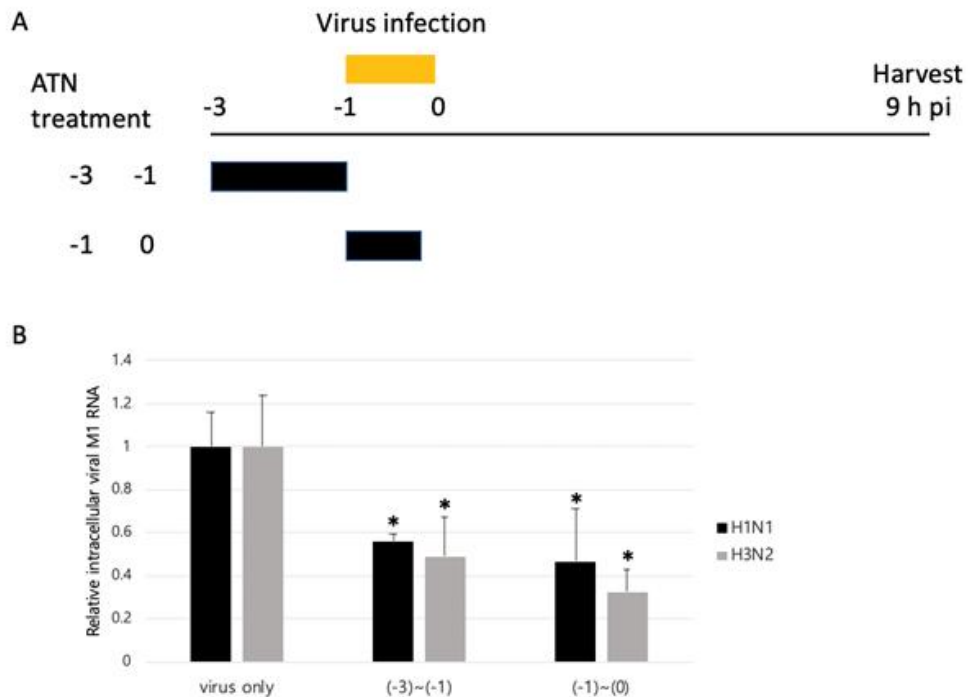


Figure 11. ATN inhibits viral RNA synthesis at an early stage of infection.

(A) Schematic diagram of ATN treatment. MDCK cells were infected with H1N1, H3N2 (MOI = 0.1) and treated with ATN (1 mg/ml). All supernatants were collected at 9 h pi. (B) Viral RNA expression was detected by real-time PCR using specific primers for M1 protein. *: $p < 0.05$ compared to the virus only group (n=3).

IV. DISCUSSION

Many modern drugs have been developed by verifying the effect of traditionally used natural products. Verification of the therapeutic effects of a large number of natural substances, that are widely used in Asia as traditional remedies, can be an important starting point for the designing of new drugs. While traditional medicinal substances might have higher chances of being clinically safer than the novel phytochemicals, the identification of their definitive active ingredients remains challenging as their chemical composition may differ based on geographical location and the source of origin.

Dentin regeneration using stem cells was mainly studied using dental follicle stem cells (DFSCs), dental pulp stem cells (DPSCs) and stem cells from apical papilla (SCAP) (25, 29, 30). Human periodontal ligament stem cells (hPDLSCs) have been previously studied for cementum and PDL regeneration (29, 31, 32), and a few studies report the regeneration of dentin using hPDLSCs. In a recent study comparing hPDLSCs with DFSCs, the regeneration of dentin was observed when hPDLSCs was transplanted with treated dentin matrix (TDM) (33); the examination of the harvested grafts showed that hPDLSCs formed dentin-like tissues similar to those formed by DFSCs. However, the structure of dentin tissues generated by DFSCs was observed to be more complete. It seems that the microenvironment of TDM plays a pivotal role in the dentin regeneration of hPDLSCs (25). In the present study, the efficacy of ATN was evaluated by dentinogenesis-associated genes. The expression of odontoblastic differentiation-related genes, such as DMP1 and DSPP, was upregulated as determined using real-time PCR and western blot analysis. These results

suggest the possibility of dentin regeneration by ATN. DMP-1 is a member of the SIBLING family whose expression is enhanced by mechanical loading in osteocytes (34). DMP-1 knockout results in hypomineralization due to elevated FGF-23 production (35). Although DMP-1 was originally thought to be specific to dentin, it has been subsequently found to be synthesized by osteoblasts as well (36). Also, DSPP and/or its cleaved products DSP and DPP which were previously believed to be dentin-specific, have been recently shown to be expressed in bone, cementum, and some non-mineralized tissues (37). Nevertheless, many studies suggest that these markers play an important role in the formation of dentin (38-40).

In the current study, the dentinogenic functions of ATN were investigated in an *in vivo* environment by implanting ATN-treated hPDLSCs into mice at a site with no mineralization capacity. An inductive scaffold of TDM was used to achieve dentin regeneration with hPDLSCs *in vivo*. However, there were no significant differences between the control group and the ATN-treated group. In the control group, hard tissue regeneration was rarely observed which contradicts the results of a previous study (33). These results show that even if hard tissue regeneration is observed in the ATN-treated group, the results are unreliable. Similar studies using DFSCs have reported that implantation, immediately after seeding DFSCs to the TDM, did not show a satisfactory result (37). In the present study, hPDLSCs were implanted into the mouse on the next day of seeding to the TDM. Therefore, there is a possibility that hPDLSCs were transplanted without enough differentiation. Furthermore, multinucleated cells were observed around TDM, and absorption of some dentin was also suspected. This may be attributed to the death of hPDLSCs due to

inflammatory reactions.

Previous reports have shown that hPDLSCs have the potential to differentiate into osteoblasts. Multipotential availability was confirmed in this study. When PDLSCs were implanted into periodontal defects in an *in vivo* study, PDL-like tissue formation and bone regeneration were identified (41). Furthermore, enamel matrix derivative and ET-1 were reported to promote the osteoblastic differentiation of hPDLSCs (42, 43). In the present study, the influence of ATN on osteoblastic differentiation of hPDLSCs was evaluated. The results of Alizarin red S staining showed that the calcium deposition was increased after 2 weeks of incubation in the osteogenic induction medium treated with ATN. The mRNA expression of osteoblastic differentiation-related genes such as ALP, Coll1, and OPN were upregulated using real-time PCR, and western blot analysis with ATN showed an increased level of expression of OCN, BSP, and Runx2. Furthermore, OSX gene over-expressed HEK 293 cells showed a tendency of increasing BSP promoter activity compared to the control group. Runx-2 is the bone-specific transcription factor and has a major impact on osteoblast differentiation (44, 45). Phosphorylation of Runx2 is a major factor in increasing the various gene expression for osteoblast differentiation (46). ATN can regulate osteoblast differentiation through phosphorylation. Additionally, OCN and BSP are also osteoblast-specific markers, and they are present during the late stages of osteoblast differentiation. Therefore, the upregulation of OCN and BSP expression indicate an ATN-induced maturation of osteoblasts. In this study, the changes in osteoblastic differentiation related genes expression suggest that ATN could promote the osteoblastic differentiation of hPDLSCs. Combining the results of this study, it is evident that ATN could promote

osteo/odontoblastic differentiation. It will be difficult to assess the two effects separately because of the overlapping expression of the genes involved in osteogenesis and odontogenesis. Moreover, further *in vivo* studies are needed to confirm the process of differentiation.

M2 channel inhibitors and neuraminidase inhibitors are approved antiviral drugs available at present (21). The recent emergence of viruses resistant to these drugs has raised concerns about new potentially pandemic influenza strains (22, 23). Therefore, it is necessary to develop a new antiviral agent without resistance. Antiviral activity of ATN which has been known to have anti-flu property were evaluated in the current study.

ATN was shown to have an inhibitory effect against H1N1 and H3N2. The results of the time-of-addition assay indicated that ATN inhibited early stages of the influenza virus (H1N1). It is hypothesized that ATN may interfere with virus binding because pre-treatment of ATN has adequate antiviral effect. However, ATN alone does not appear to bind with the RBCs. Therefore, ATN would not attach to the HA receptor of the host cell. Rather, it is thought to cause a change in the binding site of the cell surface. HA is cleaved to HA1 and HA2. HA1 is responsible for cell-virus binding. HA2 catalyzes fusion/genome uncoating by membrane fusion at an early stage of replication. Influenza virus-ATN binding assay showed that ATN can reduce influenza virus(H1N1)-induced RBC agglutination (Fig. 8B) suggesting that ATN may bind to the HA receptor-binding region (HA1).

Antiviral drugs that target the genetically consistent HA2 proteins (i.e. the stem region of HA proteins) of influenza viruses, have been widely studied (47-49). Antiviral drugs inhibiting virus attachment have also been developed, for

example, the drugs that disable the sialic acid present on the respiratory epithelial cell surface inhibiting the binding of the virus to the host cell's surface receptors (50). Using a similar mechanism, ATN may suppress viruses by inhibiting the cell to virus interaction. At this point of time, it is difficult to know what are the active components of ATN that are involved in this mechanism. Further studies are need to identify and characterize the components of ATN to aid the development of new ATN-based antiviral drugs.

V. CONCLUSIONS

Angelica tenuissima Nakai (ATN) is a traditional medicine used to treat toothache, and flu-like symptoms. However, no research has been conducted on these therapeutic effects of ATN. In this study, periodontal tissue regeneration ability and antiviral property of ATN were investigated *in vitro*. The results of current study confirmed that

- 1) ATN has no cytotoxicity and does not affect cell migration of hPDLSCs.
- 2) ATN promotes osteoblastic/odontoblastic differentiation of hPDLSCs *in vitro*, as shown in real-time PCR and Western blot. ATN treated hPDLSCs increased osteoblastic/odontoblastic differentiation markers such as ALP, BSP, COL1, OCN, OPN, DMP1, DSPP and Runx2.
- 3) ATN shows the antiviral property against the influenza virus at the early stages of viral infection.
- 4) As a clinical implication, these results indicating ATN's potential use for periodontal tissue regeneration and anti-influenza treatment.

VI. REFERENCES

1. Ahn SJ, Baek JM, Cheon YH, Park SH, Lee MS, Oh J, et al. The Inhibitory Effect of *Angelica tenuissima* Water Extract on Receptor Activator of Nuclear Factor- κ B Ligand-Induced Osteoclast Differentiation and Bone Resorbing Activity of Mature Osteoclasts. *Am J Chin Med*. 2015;43(4):715-29.
2. Lee SH, Choi H, Kim H, Lee H, Sung YH, Kim SE, et al. Inhibitory effect of *Angelicae Tenuissimae Radix* on expressions of cyclooxygenase-2 and inducible nitric oxide synthase in mouse BV2 microglial cells. *Neurol Res*. 2010;32 Suppl 1:58-63.
3. Bae N, Ahn T, Chung S, Oh MS, Ko H, Oh H, et al. The neuroprotective effect of modified Yeoldahanso-tang via autophagy enhancement in models of Parkinson's disease. *J Ethnopharmacol*. 2011;134(2):313-22.
4. Ka MH, Choi EH, Chun HS, Lee KG. Antioxidative activity of volatile extracts isolated from *Angelica tenuissimae* roots, peppermint leaves, pine needles, and sweet flag leaves. *J Agric Food Chem*. 2005;53(10):4124-9.
5. Lee SM, Kim HJ, Jang YP. Chemometric classification of morphologically similar Umbelliferae medicinal herbs by DART-TOF-MS fingerprint. *Phytochem Anal*. 2012;23(5):508-12.
6. Yook CS, Kang CK, Inn MK, Kim KO, Kim CW. The

essential oils of *Ligusticum tenuissimum* Roots. *Yakhak Hoeji*. 1997;41(2):27-30.

7. Park HK, Lee SI, Lee SH, Park HM, Rhee JS. A study on the qualitative and quantitative analysis of essential oil in *Angelicae tenuissimae* Radix or *Ligustici rhizoma*. . *Korean JFood sci Technol* 1997;29(2):189-94.

8. Kim EO, Min KJ, Kwon TK, Um BH, Moreau RA, Choi SW. Anti-inflammatory activity of hydroxycinnamic acid derivatives isolated from corn bran in lipopolysaccharide-stimulated Raw 264.7 macrophages. *Food Chem Toxicol*. 2012;50(5):1309-16.

9. Li X, Wu D, Hu Z, Xuan J, Ding X, Zheng G, et al. The Protective Effect of Ligustilide in Osteoarthritis: An in Vitro and in Vivo Study. *Cell Physiol Biochem*. 2018;48(6):2583-95.

10. Lin JJ, Du Y, Cai WK, Kuang R, Chang T, Zhang Z, et al. Toll-like receptor 4 signaling in neurons of trigeminal ganglion contributes to nociception induced by acute pulpitis in rats. *Sci Rep*. 2015;5:12549.

11. Pihlstrom BL, Michalowicz BS, Johnson NW. Periodontal diseases. *Lancet*. 2005;366(9499):1809-20.

12. Hu L, Liu Y, Wang S. Stem cell-based tooth and periodontal regeneration. *Oral Dis*. 2018;24(5):696-705.

13. Chen FM, Gao LN, Tian BM, Zhang XY, Zhang YJ, Dong GY, et al. Treatment of periodontal intrabony defects using

autologous periodontal ligament stem cells: a randomized clinical trial. *Stem Cell Res Ther.* 2016;7:33.

14. Chen FM, Sun HH, Lu H, Yu Q. Stem cell-delivery therapeutics for periodontal tissue regeneration. *Biomaterials.* 2012;33(27):6320-44.

15. Bright R, Hynes K, Gronthos S, Bartold PM. Periodontal ligament-derived cells for periodontal regeneration in animal models: a systematic review. *J Periodontal Res.* 2015;50(2):160-72.

16. Seo BM, Miura M, Gronthos S, Bartold PM, Batouli S, Brahimi J, et al. Investigation of multipotent postnatal stem cells from human periodontal ligament. *Lancet.* 2004;364(9429):149-55.

17. Zhu W, Liang M. Periodontal ligament stem cells: current status, concerns, and future prospects. *Stem Cells Int.* 2015;2015:972313.

18. Webster RG, Bean WJ, Gorman OT, Chambers TM, Kawaoka Y. Evolution and ecology of influenza A viruses. *Microbiol Rev.* 1992;56(1):152-79.

19. Memoli MJ, Morens DM, Taubenberger JK. Pandemic and seasonal influenza: therapeutic challenges. *Drug Discov Today.* 2008;13(13-14):590-5.

20. Lambert LC, Fauci AS. Influenza vaccines for the future. *N Engl J Med.* 2010;363(21):2036-44.

21. Sugrue RJ, Tan BH, Yeo DS, Sutejo R. Antiviral drugs for the control of pandemic influenza virus. *Ann Acad Med Singapore*. 2008;37(6):518-24.
22. Fedson DS. Confronting an influenza pandemic with inexpensive generic agents: can it be done? *Lancet Infect Dis*. 2008;8(9):571-6.
23. Moss RB, Davey RT, Steigbigel RT, Fang F. Targeting pandemic influenza: a primer on influenza antivirals and drug resistance. *J Antimicrob Chemother*. 2010;65(6):1086-93.
24. Lin TJ, Lin CF, Chiu CH, Lee MC, Horng JT. Inhibition of endosomal fusion activity of influenza virus by *Rheum tanguticum* (da-huang). *Sci Rep*. 2016;6:27768.
25. Li R, Guo W, Yang B, Guo L, Sheng L, Chen G, et al. Human treated dentin matrix as a natural scaffold for complete human dentin tissue regeneration. *Biomaterials*. 2011;32(20):4525-38.
26. Parolini O, Alviano F, Bagnara GP, Bilic G, Buhring HJ, Evangelista M, et al. Concise review: isolation and characterization of cells from human term placenta: outcome of the first international Workshop on Placenta Derived Stem Cells. *Stem Cells*. 2008;26(2):300-11.
27. Xu J, Wang W, Kapila Y, Lotz J, Kapila S. Multiple differentiation capacity of STRO-1+/CD146+ PDL mesenchymal progenitor cells. *Stem Cells Dev*. 2009;18(3):487-96.

28. Dominici M, Le Blanc K, Mueller I, Slaper-Cortenbach I, Marini F, Krause D, et al. Minimal criteria for defining multipotent mesenchymal stromal cells. The International Society for Cellular Therapy position statement. *Cytotherapy*. 2006;8(4):315-7.
29. Shi S, Bartold PM, Miura M, Seo BM, Robey PG, Gronthos S. The efficacy of mesenchymal stem cells to regenerate and repair dental structures. *Orthod Craniofac Res*. 2005;8(3):191-9.
30. Jin B, Choung PH. Recombinant Human Plasminogen Activator Inhibitor-1 Accelerates Odontoblastic Differentiation of Human Stem Cells from Apical Papilla. *Tissue Eng Part A*. 2016;22(9-10):721-32.
31. Jin H, Choung HW, Lim KT, Jin B, Jin C, Chung JH, et al. Recombinant Human Plasminogen Activator Inhibitor-1 Promotes Cementogenic Differentiation of Human Periodontal Ligament Stem Cells. *Tissue Eng Part A*. 2015;21(23-24):2817-28.
32. Park JY, Park CH, Yi T, Kim SN, Iwata T, Yun JH. rhBMP-2 Pre-Treated Human Periodontal Ligament Stem Cell Sheets Regenerate a Mineralized Layer Mimicking Dental Cementum. *Int J Mol Sci*. 2020;21(11):3767
33. Tian Y, Bai D, Guo W, Li J, Zeng J, Yang L, et al. Comparison of human dental follicle cells and human periodontal ligament cells for dentin tissue regeneration. *Regen Med*. 2015;10(4):461-79.

34. Harris SE, Gluhak-Heinrich J, Harris MA, Yang W, Bonewald LF, Riha D, et al. DMP1 and MEPE expression are elevated in osteocytes after mechanical loading in vivo: theoretical role in controlling mineral quality in the perilacunar matrix. *J Musculoskelet Neuronal Interact.* 2007;7(4):313-5.
35. Feng JQ, Ward LM, Liu S, Lu Y, Xie Y, Yuan B, et al. Loss of DMP1 causes rickets and osteomalacia and identifies a role for osteocytes in mineral metabolism. *Nat Genet.* 2006;38(11):1310-5.
36. D'Souza RN, Cavender A, Sunavala G, Alvarez J, Ohshima T, Kulkarni AB, et al. Gene expression patterns of murine dentin matrix protein 1 (Dmp1) and dentin sialophosphoprotein (DSPP) suggest distinct developmental functions in vivo. *J Bone Miner Res.* 1997;12(12):2040-9.
37. Prasad M, Butler WT, Qin C. Dentin sialophosphoprotein in biomineralization. *Connect Tissue Res.* 2010;51(5):404-17.
38. Quispe-Salcedo A, Ida-Yonemochi H, Nakatomi M, Ohshima H. Expression patterns of nestin and dentin sialoprotein during dentinogenesis in mice. *Biomed Res.* 2012;33(2):119-32.
39. Sreenath T, Thyagarajan T, Hall B, Longenecker G, D'Souza R, Hong S, et al. Dentin sialophosphoprotein knockout mouse teeth display widened predentin zone and develop defective dentin mineralization similar to human dentinogenesis imperfecta type III. *J Biol Chem.* 2003;278(27):24874-80.

40. Xiao S, Yu C, Chou X, Yuan W, Wang Y, Bu L, et al. Dentinogenesis imperfecta 1 with or without progressive hearing loss is associated with distinct mutations in DSPP. *Nat Genet.* 2001;27(2):201-4.
41. Liu Y, Zheng Y, Ding G, Fang D, Zhang C, Bartold PM, et al. Periodontal ligament stem cell-mediated treatment for periodontitis in miniature swine. *Stem Cells.* 2008;26(4):1065-73.
42. Kato H, Katayama N, Taguchi Y, Tominaga K, Umeda M, Tanaka A. A synthetic oligopeptide derived from enamel matrix derivative promotes the differentiation of human periodontal ligament stem cells into osteoblast-like cells with increased mineralization. *J Periodontol.* 2013;84(10):1476-83.
43. Liang L, Zhou W, Yang N, Yu J, Liu H. ET-1 Promotes Differentiation of Periodontal Ligament Stem Cells into Osteoblasts through ETR, MAPK, and Wnt/beta-Catenin Signaling Pathways under Inflammatory Microenvironment. *Mediators Inflamm.* 2016;2016:8467849.
44. Choi YH, Han Y, Jin SW, Lee GH, Kim GS, Lee DY, et al. Pseudoshikonin I enhances osteoblast differentiation by stimulating Runx2 and Osterix. *J Cell Biochem.* 2018;119(1):748-57.
45. Harada S, Rodan GA. Control of osteoblast function and regulation of bone mass. *Nature.* 2003;423(6937):349-55.
46. Ren D, Wei F, Hu L, Yang S, Wang C, Yuan X.

Phosphorylation of Runx2, induced by cyclic mechanical tension via ERK1/2 pathway, contributes to osteodifferentiation of human periodontal ligament fibroblasts. *J Cell Physiol.* 2015;230(10):2426–36.

47. Oh HL, Akerstrom S, Shen S, Bereczky S, Karlberg H, Klingstrom J, et al. An antibody against a novel and conserved epitope in the hemagglutinin 1 subunit neutralizes numerous H5N1 influenza viruses. *J Virol.* 2010;84(16):8275–86.

48. Ekiert DC, Wilson IA. Broadly neutralizing antibodies against influenza virus and prospects for universal therapies. *Curr Opin Virol.* 2012;2(2):134–41.

49. Fleishman SJ, Whitehead TA, Ekiert DC, Dreyfus C, Corn JE, Strauch EM, et al. Computational design of proteins targeting the conserved stem region of influenza hemagglutinin. *Science.* 2011;332(6031):816–21.

50. Belser JA, Lu X, Szretter KJ, Jin X, Aschenbrenner LM, Lee A, et al. DAS181, a novel sialidase fusion protein, protects mice from lethal avian influenza H5N1 virus infection. *J Infect Dis.* 2007;196(10):1493–9.

국문초록

한고본: 사람치주인대 줄기세포의 조골세포/조상아세포 분화 촉진 효과 및 인플루엔자 바이러스에 대한 항바이러스 성질, 시험관 내 연구

서울대학교 대학원 치의과학과 구강악안면외과
(지도교수 : 정 필 훈)

박 원 중

1. 목 적

한고본은 치통, 두통, 감기증상의 치료에 사용되는 한약재로 그 효과에 대한 연구가 자세히 이루어지지 않았다. 특히 치통과 감기증상 치료에 대한 근거는 확실하지 않은 상태이다. 본 논문은 한고본이 지니는 이 효능에 대해 규명하고자 두 가지 방법으로 연구를 진행하였다.

치주질환은 가장 흔한 만성질환으로 이를 치료하기 위해 많은 연구가 이루어져 왔다. 치주조직은 치통을 일으키는 가장 흔한 원인으로 치조골 파괴를 동반하여 동통을 유발한다. 한고본이 파괴된 경조직 재생효과를 통해 통증을 조절할 것이라는 가설 하에 사람치주인대줄기세포를 이용하

여 한고본의 효과를 알아보았다.

한고본은 감기의 치료에 이용되는 약물로서 그 기전을 살펴보기 위해 influenza virus에 대한 항바이러스효과를 검증하고자 하였다.

2. 방 법

성인에서 발치된 제3대구치의 치주인대 조직에서 줄기세포를 얻었다. 배양한 줄기세포를 유세포 분석과 골모세포, 연골세포, 지방세포로의 분화를 통하여 줄기세포 표지자 및 다분화능을 확인하였다.

Cell proliferation 에 미치는 영향을 보기위해 MTT test와 Cell migration test를 시행하였으며 독성을 가지지 않는 여러 농도에서 골분화를 유도 하였다. Alizarin red staining 염색을 통해 광화를 확인하였고 이후 real-time PCR 및 western blot을 통해 다양한 표지자를 확인하였다. Osterix를 과발현한 세포에 한고본이 미치는 영향을 확인하기 위해 형질주입과 발광효소 분석을 시행하였다.

동물실험을 위해 누드마우스의 피하에 한고본을 처리하거나 처리하지 않은 치주인대 줄기세포와 treated dentin matrix을 이식하고 8주 뒤에 H&E stain을 통해 효과를 확인하였다.

H1N1, H3N2 virus에서 한고본의 항바이러스 효과를 보기위해 MDCK cell 에 MTT assay를 시행하고 CC₅₀을 구하였으며 바이러스 역가 측정을 위해 Hemagglutination inhibition assay와 TCID₅₀를 시행하였다. time of addition assay, microscopic examination, influenza virus-ATN binding assay, real-time PCR 이 시행되었다.

3. 결 과

사람치주인대줄기세포에 대해 유세포 분석을 시행한결과 중간엽 유래

줄기세포의 표지자(CD13⁺, CD90⁺, CD146⁺, CD34⁻)를 확인하였으며 분화 유도를 시행했을 때 골조직, 연골조직, 지방조직으로 분화가 가능함을 확인하였다. MTT assay에서 200 µg/mL 까지는 세포독성이 나타나지 않았으며 Cell migration test에서는 대조군과 특별한 차이는 보이지 않았다. 또한 100 µg/mL의 농도에서 치주인대줄기세포의 광화가 더 촉진되었다. real-time PCR을 시행하였을 때 Alkaline Phosphatase(ALP), Dentin Matrix protein (DMP1), type 1 collagen (COL1), Osteopontin (OPN), Dentin Sialophosphoprotein(DSPP)의 증가를 확인하였다. Western blot 에서는 osteocalcin (OCN), dentin sialophosphoprotein (DSPP), dentin matrix protein (DMP1), Runt-related transcription factor 2 (Runx2) 단백질이 증가하였다. 형질주입과 발광효소분석에서는 Osterix DNA를 과활성화한 293 cell에 한고본을 처리했을 때 Bone Sialoprotein (BSP) promotor 활성이 증가하는 경향을 확인하였다. 누드 마우스를 이용한 동물실험에서는 대조군과 실험군 모두에서 골화는 관찰되지 않았다.

ATN은 H1N1, H3N2 virus에 대해서 항바이러스 성질을 나타내었다. 현미경 결과에서 더 많은 세포가 살아남음을 확인하였고 바이러스 처리 전에 ATN을 처리한 그룹에서 전 기간 동안 처리한 그룹과 유사한 억제 효과를 보여주었다. 바이러스 처리 전, 바이러스와 동시에 ATN을 처리한 군에서 대조군보다 낮은 viral RNA(M1 protein) 수준을 보여주었다.

4. 결 론

한고본은 사람치주인대 줄기세포의 조골세포/조상아세포 분화 촉진 효과를 나타냈으며 인플루엔자 바이러스에 대해서 항바이러스 성질을 보여주었다.

주요어 : 한고본, 사람치주인대 줄기세포, 조골세포/조상아세포 분화 촉진, 항바이러스, 인플루엔자 바이러스

학 번 : 2011-31174